

A 1:1:1 co-crystal solvate comprising 2,2'-dithiodibenzoic acid, 2-chlorobenzoic acid and *N,N*-dimethylformamide: crystal structure, Hirshfeld surface analysis and computational study

Sang Loon Tan and Edward R. T. Tiekink*

Received 6 March 2019

Accepted 19 March 2019

Research Centre for Crystalline Materials, School of Science and Technology, Sunway University, 47500 Bandar Sunway, Selangor Darul Ehsan, Malaysia. *Correspondence e-mail: edwardt@sunway.edu.my

Edited by W. T. A. Harrison, University of Aberdeen, Scotland

Keywords: crystal structure; dithiodibenzoic acid; chlorobenzoic acid; hydrogen bonding; Hirshfeld surface analysis; computational chemistry.

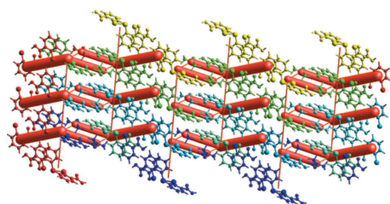
CCDC reference: 1903993

Supporting information: this article has supporting information at journals.iucr.org/e

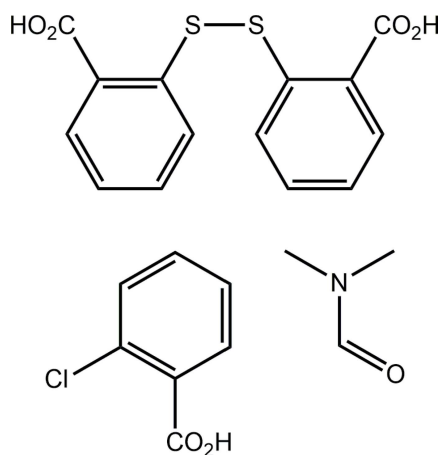
The asymmetric unit of the three-component title compound, 2,2'-dithiodibenzoic acid–2-chlorobenzoic acid–*N,N*-dimethylformamide (1/1/1), $C_{14}H_{10}O_4S_2 \cdot C_7H_5ClO_2 \cdot C_3H_7NO$, contains a molecule each of 2,2'-dithiodibenzoic acid (DTBA), 2-chlorobenzoic acid (2CBA) and dimethylformamide (DMF). The DTBA molecule is twisted [the C–S–S–C torsion angle is $88.37(17)^\circ$] and each carboxylic group is slightly twisted from the benzene ring to which it is connected [CO_2/C_6 dihedral angles = $7.6(3)$ and $12.5(3)^\circ$]. A small twist is evident in the molecule of 2CBA [CO_2/C_6 dihedral angle = $4.4(4)^\circ$]. In the crystal, the three molecules are connected by hydrogen bonds with the two carboxylic acid residues derived from DTBA and 2CBA forming a non-symmetric eight-membered $\{\cdots HOCO\}_2$ synthon, and the second carboxylic acid of DTBA linked to the DMF molecule *via* a seven-membered $\{\cdots HOCO\cdots HCO\}$ heterosynthon. The three-molecule aggregates are connected into a supramolecular chain along the *a* axis *via* DTBA–C–H \cdots O(hydroxyl-2CBA), 2CBA–C–H \cdots O(hydroxyl-DTBA) and DTBA–C–H \cdots S(DTBA) interactions. Supramolecular layers in the *ab* plane are formed as the chains are linked *via* DMF–C–H \cdots S(DTBA) contacts, and these interdigitate along the *c*-axis direction without specific points of contact between them. A Hirshfeld surface analysis points to additional but, weak contacts to stabilize the three-dimensional architecture: DTBA–C=O \cdots H(phenyl-DTBA), 2CBA–Cl \cdots H(phenyl-DTBA), as well as a π – π contact between the delocalized eight-membered $\{\cdots HOC=O\}_2$ carboxylic dimer and the phenyl ring of 2CBA. The latter was confirmed by electrostatic potential (ESP) mapping.

1. Chemical context

Recent bibliographic reviews have highlighted the rich coordination chemistry based on ligands derived from 2-mercaptobenzoic acid (2-MBA) (Wehr-Candler & Henderson, 2016) and its 3- and 4-isomeric analogues (Tiekink & Henderson, 2017). By contrast, co-crystal formation with these molecules is quite limited with the only co-crystal of an *n*-MBA molecule being that formed between 2-MBA and its oxidation product 2,2'-dithiodibenzoic acid (DTBA) (Rowland *et al.*, 2011). One reason for the scarcity of co-crystals containing 2-MBA is the propensity for the acid to be oxidized, to generate DTBA, during co-crystallization experiments with bipyridyl-type molecules (Broker & Tiekink, 2007) and with other carboxylic acids (Tan & Tiekink, 2019*a*). Another, less common, outcome of crystallization experiments with 2-MBA is the sulfur extrusion product, 2,2'-thiodibenzoic acid (Tan & Tiekink, 2018; Gorobet *et al.*, 2018). Herein,



another unexpected product from a co-crystallization experiment involving 2-MBA is described. While the now anticipated coformer DTBA was observed after the co-crystallization of 2-MBA with 2-chlorobenzoic acid (2CBA), and recrystallization from a toluene/dimethylformamide solution (50:50 *v/v*), a solvent dimethylformamide molecule was also found in the resultant co-crystal solvate. In this three-component crystal, one of the carboxylic acid groups of the DTBA molecule forms hydrogen bonds to DMF rather than to 2CBA. Herein, the crystal and molecular structures of the title co-crystal solvate are described along with an analysis of the calculated Hirshfeld surfaces and a computational chemistry study.



2. Structural commentary

The title compound, (I), was isolated from the co-crystallization of 2-mercaptobenzoic acid and 2-chlorobenzoic acid prepared through solvent-assisted (methanol) grinding, followed by recrystallization from a toluene/dimethylformamide solution (50:50 *v/v*). The asymmetric unit comprises 2,2'-dithiodibenzoic acid (DTBA), 2-chlorobenzoic acid (2CBA) and a dimethylformamide (DMF) solvent molecule in a stoichiometric 1:1:1 ratio, as illustrated in Fig. 1; each molecule is in a general position.

As anticipated, crystallography reveals that the original 2-mercaptobenzoic acid underwent oxidation to yield a molecule of DTBA, with the benzoic acid moieties being bridged through a disulfide bond [$S1-S2 = 2.053(1) \text{ \AA}$]. The presence of carboxylic acid groups is confirmed by the disparity in the bond lengths for $C8-O4$, $O3$ [$1.317(4)$ and $1.229(4) \text{ \AA}$] and $C21-O6$, $O5$ [$1.326(4)$ and $1.209(4) \text{ \AA}$]. Both carboxylic acid groups ($O3-C8-O4$ and $O5-C21-O6$) are slightly twisted from the benzene rings ($C9/C14$ and $C15/C20$) to which they are bonded with the corresponding dihedral angles being $7.6(3)^\circ$ and $12.5(3)^\circ$, respectively. The $C14-S1-S2-C15$ torsion angle is $88.37(17)^\circ$, indicating an almost orthogonal disposition between the benzene rings. The carbonyl- $O3$ and $O5$ atoms are oriented towards the disulfide- $S1$ and $S2$ atoms with $S1 \cdots O3$ and $S2 \cdots O5$ distances of $2.713(2)$ and $2.661(3) \text{ \AA}$, respectively, and are indicative of hypervalent $S \leftarrow O$ interactions (Nakanishi *et al.*, 2007).

Table 1
Hydrogen-bond geometry (\AA , $^\circ$).

$D-H \cdots A$	$D-H$	$H \cdots A$	$D \cdots A$	$D-H \cdots A$
$O2-H2O \cdots O3$	0.83 (6)	1.86 (7)	2.687 (4)	176 (9)
$O4-H4O \cdots O1$	0.73 (7)	1.88 (6)	2.612 (4)	175 (5)
$O6-H6O \cdots O7$	0.87 (5)	1.73 (5)	2.594 (4)	172 (5)
$C3-H3 \cdots O4^i$	0.95	2.57	3.363 (5)	142
$C10-H10 \cdots O2^{ii}$	0.95	2.54	3.331 (5)	141
$C11-H11 \cdots S1^{ii}$	0.95	2.83	3.544 (4)	133
$C22-H22 \cdots O5$	0.95	2.33	3.095 (5)	138
$C24-H24B \cdots S2^{iii}$	0.98	2.83	3.531 (4)	129

Symmetry codes: (i) $x-1, y, z$; (ii) $x+1, y, z$; (iii) $-x+1, -y, -z+1$.

As for DTBA, the confirmation that 2CBA exists as a carboxylic acid is readily ascertained by the difference observed in the $C1-O1$, $O2$ bond lengths of $1.222(4)$ and $1.320(4)$, respectively. The carboxylic acid group is almost coplanar with the phenyl ring ($C2-C7$) as seen in the dihedral angle of $4.4(4)^\circ$ between their planes. Similarly, co-planarity is also noted between the chloride atom and benzene ring plane with the r.m.s deviation from the least-squares plane through the seven non-hydrogen atoms being 0.027 \AA .

3. Supramolecular features

The geometric parameters characterizing the interatomic contacts in the crystal of (I), as identified in *PLATON* (Spek, 2009), are given in Table 1. Some of the main contacts in the molecular packing provide direct links between DTBA, 2CBA and DMF molecules, in that hydrogen bonds are formed between one of the terminal carboxylic groups of DTBA and 2CBA, and between the other carboxylic acid terminus with the carbonyl group of DMF. The former interaction leads to a

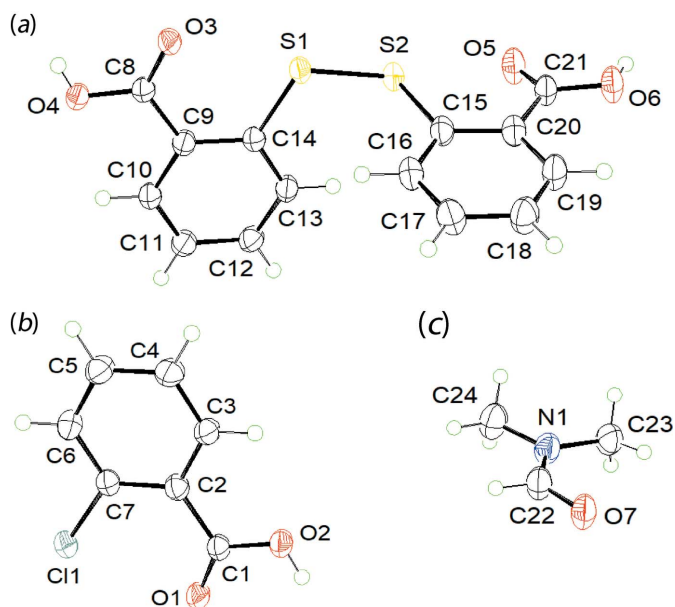


Figure 1
The molecular structures of (a) 2,2'-dithiodibenzoic acid, (b) 2-chlorobenzoic acid and (c) dimethylformamide in (I), showing the atom-labelling scheme and displacement ellipsoids at the 50% probability level.

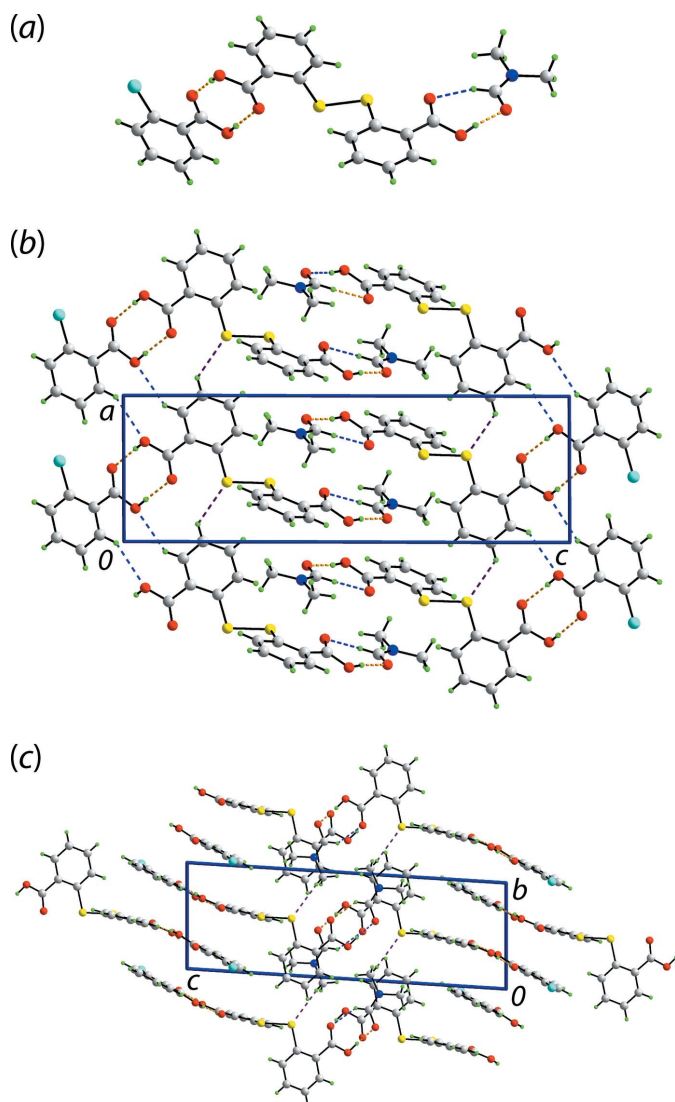


Figure 2

Molecular packing in (I): (a) a view of the three-molecule aggregate with the O—H \cdots O hydrogen bonds and C—H \cdots O interactions shown as orange and blue dashed lines, respectively, (b) supramolecular chains aligned along the *a* axis with the C—H \cdots S interactions shown as purple dashed lines and (c) a view of the unit-cell contents in perspective down the *a* axis.

classical, but non-symmetric eight-membered $\{\cdots\text{HOCO}\}_2$ homosynthon while the latter results in a seven-membered $\{\cdots\text{HOCO}\cdots\text{HCO}\}$ heterosynthon when the C22—H22 \cdots O5 interaction is taken into account, Fig. 2(a).

The resultant three-molecule aggregates are connected by DTBA-C10—H10 \cdots O2(hydroxyl-2CBA) and 2CBA-C3—H3 \cdots O4(hydroxyl-DTBA) interactions to form a non-symmetric, ten-membered $\{\cdots\text{OCCCH}\}_2$ homosynthon, as well as discrete DTBA-C11—H11 \cdots S1(DTBA) interactions. These lead to a supramolecular chain along the crystallographic *a* direction, as indicated in Fig. 2(b). Interactions between the chains leading to a layer in the *ab* plane occur through DMF-C24—H24C \cdots S2(DTBA) contacts, Fig. 2(c). The layers inter-digitate along the *c*-axis direction with only weak contacts between them as detailed in the next section.

4. Hirshfeld surface analysis

To better understand the nature of the intermolecular interactions in the crystal of (I), the individual molecules comprising the asymmetric unit as well as the contents of the asymmetric unit were subjected to Hirshfeld surface analysis using *Crystal Explorer 17* (Turner *et al.*, 2017) and based on the procedures described in the literature (Tan *et al.*, 2019).

The d_{norm} maps of the respective molecules in the aggregates are shown in Fig. 3. DTBA exhibits several intense red spots on the d_{norm} map signifying close contacts which originate from DTBA—O—H \cdots O(carbonyl-2CBA), DTBA—O—H \cdots O(carbonyl-DMF), DTBA—C=O \cdots H(hydroxyl-2CBA) and DTBA—C=O \cdots H(DMF). Other red spots are observed through the d_{norm} map, albeit with relatively weak intensity. The contacts are consistent with those identified above except for some additional interactions such as DTBA—C=O \cdots H(phenyl-DTBA), 2CBA—Cl \cdots H(phenyl-DTBA) as well as a π — π contact between the delocalized eight-membered $\{\cdots\text{HOC=O}\}_2$ carboxylic dimer and the phenyl ring of 2CBA, Fig. 3(b). To validate the non-conventional π — π contact, the interacting molecules were subjected to electrostatic potential (ESP) mapping using *Spartan'16* (Spartan'16, 2017) by treating the DTBA dimer as a single entity through a DFT-B3LYP/6-311+G(*d,p*) level of theory. The ESP mapping shows that the dimeric ring ranges from electropositive to neutral within the centre of the ring while the phenyl ring of 2CBA is mainly neutral indicating that the interaction is mainly diffusive in nature, Fig. 3(c) and (d). As for the 2CBA and DMF molecules, the corresponding d_{norm} maps (not shown) are reflective of their interactions with the DTBA molecule.

The two-dimensional fingerprint plots were generated to quantify the close contacts identified on the Hirshfeld surfaces.

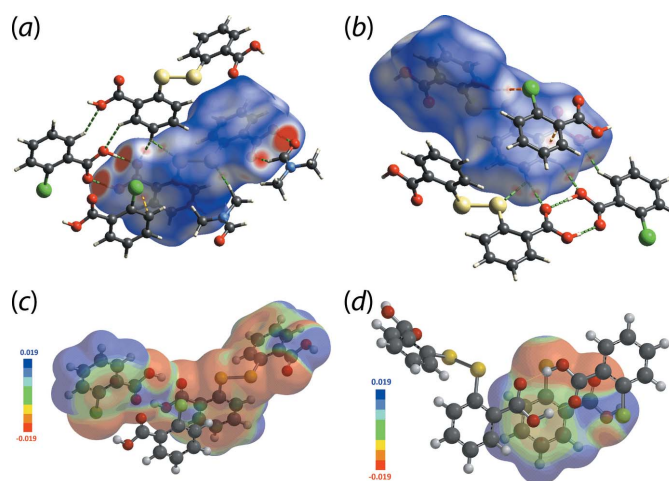


Figure 3

(a) and (b) Two views of the d_{norm} map of the DTBA molecule within the range -0.274 to $+0.862$ arbitrary units, showing the short contacts highlighted as red spots with the intensity relative to the contact distances. Hydrogen bonds are indicated as green dashed lines and π — π contacts are highlighted as yellow dashed lines. ESPs map of (c) the DTBA dimer and (d) 2CBA, with the isosurface value scaled from -0.019 to $+0.019$ atomic units.

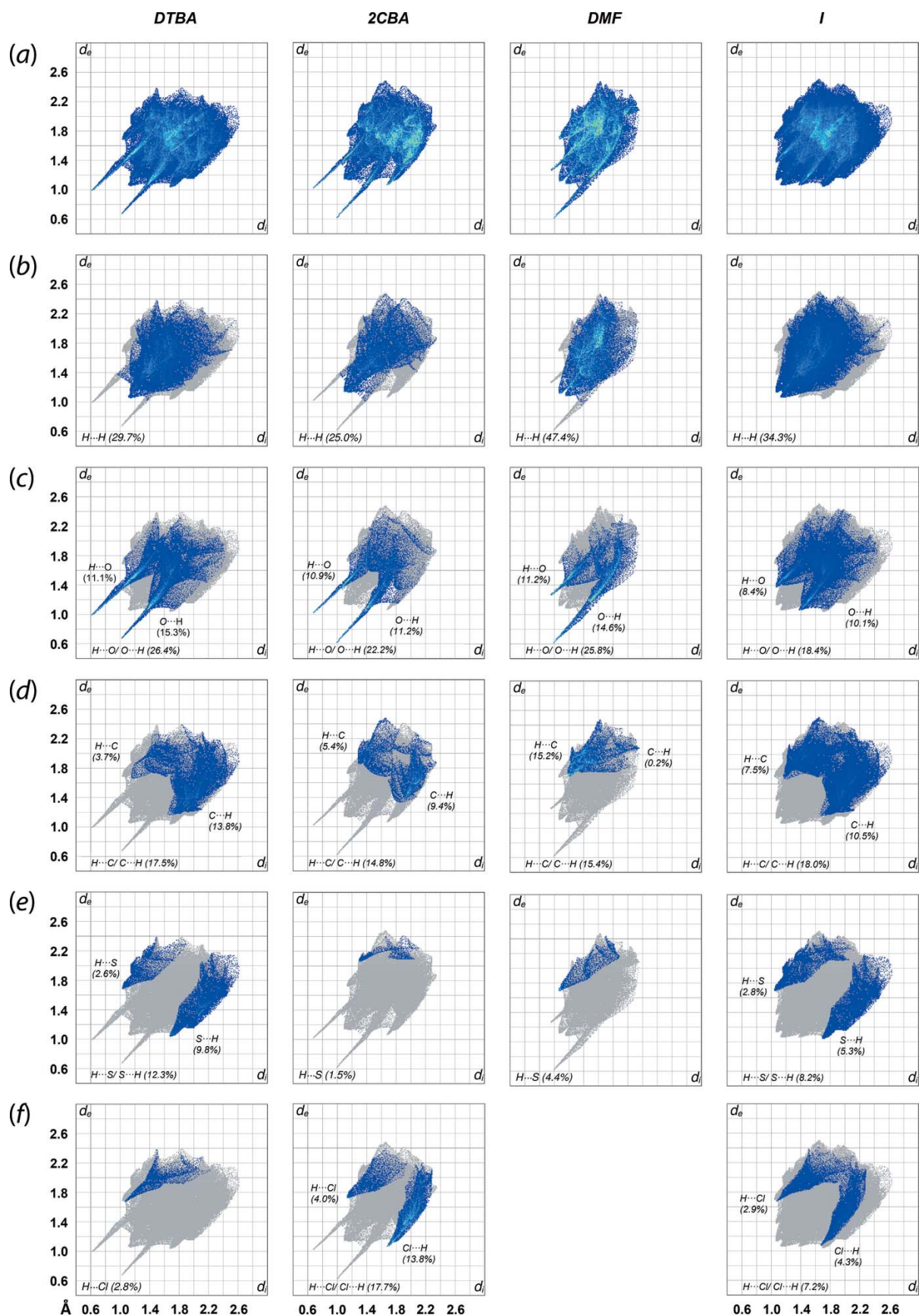


Figure 4

(a) The overall two-dimensional fingerprint plots for the DTBA, 2CBA and DMF molecules and entire (I), and those delineated into (b) H...H, (c) H...O/O...H, (d) H...C/C...H, (e) H...S/S...H and (f) H...Cl/Cl...H contacts, with the percentage contribution being specified for each contact.

Table 2

Interaction energies (kJ mol⁻¹) for selected close contacts.

Contact	$E_{\text{electrostatic}}$	$E_{\text{polarization}}$	$E_{\text{dispersion}}$	$E_{\text{exchange-repulsion}}$	E_{total}	Symmetry operation
O2—H2...O3/O4—H4O...O1	-123.7	-28.0	-13.0	145.1	-73.2	x, y, z
O6—H6O...O7/C22—H22...O5	-82.4	-19.2	-11.4	105.7	-45.9	x, y, z
Cg1(C9/C14)...Cg2(C2/C7)/C6—H16...Cl1	-4.1	-1.7	-41.9	30.3	-23.4	$1-x, 1-y, -z$
Cg3(C1O1O2...C8O3O4)...Cg2(C2/C7)	-1.0	-1.8	-30.7	21.6	-15.9	$1-x, -y, -z$
C11—H11...S1/C11—H11...O3	-11.6	-2.2	-15.0	21.3	-13.8	$-1+x, y, z$
C24—H24C...S2/C24—H24C...O5	-10.3	-2.5	-14.3	19.5	-13.2	$1-x, -y, 1-z$
C10—H10...O2/C3—H3...O4	-2.4	-1.1	-14.5	15.4	-6.5	$-x, -y, 1-z$

The overall fingerprint plot of (I) and the corresponding plots of the individual components are shown in Fig. 4. In general, (I) exhibits a shield-like profile in the overall fingerprint plot without any obvious spikes unlike the individual components. This indicates the discrete nature of the three-molecule aggregate sustained by hydrogen bonding. Decomposition of the full fingerprint plots of (I) shows that the contacts are mainly dominated by H...H (34.3%; $d_i + d_e \sim 2.20$ Å), O...H/H...O (18.4%; $d_i + d_e \sim 2.44$ Å), C...H/H...C (18.0%; $d_i + d_e \sim 2.86$ Å), S...H/H...S (8.2%; $d_i + d_e \sim 2.74$ Å), Cl...H/H...Cl (7.2%; $d_i + d_e \sim 2.72$ Å) and other contacts (14.0%). Almost all of these contacts are shorter than their corresponding sum van der Waals radii, with H...H, O...H, C...H, S...H and Cl...H being ~ 2.4 , ~ 2.72 , ~ 2.9 , ~ 3.0 and ~ 2.95 Å, respectively.

The DTBA and 2CBA molecules display similar fingerprint patterns having a claw-like profile in the respective full fingerprint plots, implying the existence of nearly identical interactions between the molecules which is expected considering the similarity of their molecular structures. Detailed analysis of the decomposed fingerprint plots shows that H...H is the most prevalent contact for the molecules, with the percentage contribution to the overall contacts of 29.7 and 25.0% and minimum $d_i + d_e$ contact distance of ~ 2.18 and ~ 2.24 Å for DTBA and 2CBA, respectively. The O...H/H...O contacts are the second most dominant contact for the individual molecules which lead to the distinctive spikes in the corresponding decomposed fingerprint plots with a contribution of 26.4% for DTBA and 22.2% for 2CBA. Further delineation of the contact shows that DTBA possesses about 11.1% of (internal)-H...O-(external) and 15.3% (internal)-O...H-(external) compared to 2CBA with 10.9 and 11.2% of the equivalent contacts, both with approximately the same $d_i + d_e$ contact distance of ~ 1.70 Å for DTBA and ~ 1.62 Å for

2CBA. Additional contacts for DTBA and 2CBA are respectively dominated by C...H/H...C (17.5%, $d_i + d_e \sim 2.18$ Å; 14.8%, $d_i + d_e \sim 3.16$ Å), S...H/H...S (12.3%, $d_i + d_e \sim 2.72$ Å; 1.5%, $d_i + d_e \sim 3.38$ Å) and Cl...H/H...Cl (2.8%, $d_i + d_e \sim 2.74$ Å; 17.7%, $d_i + d_e \sim 2.74$ Å). As for the DMF solvent molecule, this exhibits a relatively different claw-like profile with several disproportional spikes observed in the fingerprint plot mainly owing to the asymmetric interaction environment for the O...H/H...O contact, in which the contribution of (internal)-O...H-(external) contact to the Hirshfeld surfaces is about 14.6% ($d_i + d_e \sim 1.60$ Å), while the (internal)-H...O-(external) contact is about 11.2% ($d_i + d_e \sim 2.22$ Å) that can be summed up to yield an overall 25.8%. The contribution of other short contacts is noted in decreasing order: H...H (47.4%, $d_i + d_e \sim 2.20$ Å), C...H/H...C (15.4%, $d_i + d_e \sim 2.90$ Å) and H...S (4.4%, $d_i + d_e \sim 3.36$ Å), respectively.

5. Computational chemistry study

The energy calculations through *Crystal Explorer 17*, Table 2, indicate that the strongest interaction occurs between the hydrogen-bonded DTBA and 2CBA molecules [DTBA-O—H...O(carbonyl-2CBA)/DTBA=O...H—O-(hydroxyl-2CBA)] dimer with an interaction energy (E_{int}) of -73.2 kJ mol⁻¹. This energy is about one and a half-fold greater than the second strongest interaction that occurs between DTBA-DMF [DTBA-O—H...O(carbonyl-DMF)/DTBA=O...H—C-(DMF)] with an $E_{\text{int}} = -45.9$ kJ mol⁻¹. The disparity in energy is likely due the replacement of one O—H...O hydrogen bond with a C—H...O interaction in the latter interaction.

On the other hand, the π - π interaction between the hydrogen bond-mediated dimer of (DTBA)₂ and the 2CBA-

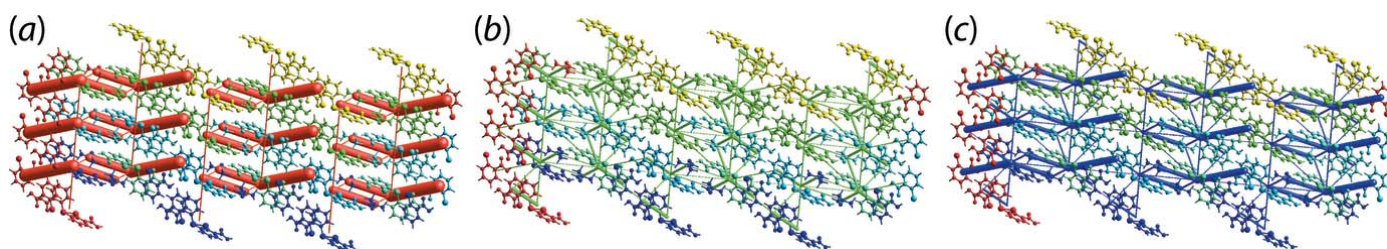


Figure 5

Energy framework of (I) as viewed down along the b axis, showing the energy framework comprising (a) electrostatic potential force, (b) dispersion force and (c) total energy. The cylindrical radii are proportional to the relative strength of the respective energies and they were scaled by a factor of 80 with a cut-off energy value of 5 kJ mol⁻¹ within $4 \times 4 \times 4$ unit cells.

benzene ring gives an energy of $-15.9 \text{ kJ mol}^{-1}$ which is considered weak in nature. This indicates the energy is mainly dominated by dispersive forces, Table 2, which validates the previous finding on ESP mapping. Interestingly, a recent study demonstrated that the presence of external agents such as Lewis acids may either increase or decrease the strength of resonance assisted hydrogen bonds (RAHB) depending on the position of interaction of the external agent with a carboxylic acid dimer (Grabowski, 2008). The E_{int} for other interactions present in the crystal were also calculated and the results are summarized as in Table 2. Generally, the energies for these interactions range between -23.4 to -6.5 kJ mol^{-1} which can be considered weak.

The energy frameworks of (I) were also generated. The results of the calculations show that the molecular packing is mainly governed by electrostatic forces which can be attributed to the strong $\text{O}-\text{H}\cdots\text{O}$ interactions, Fig. 5. The interactions coupled with the near orthogonal arrangement of the two carboxylic acid moieties of DTBA lead to a discrete, directional V-shape electrostatic energy topology which is arranged in an alternate array along the c -axis direction. A relatively weaker dispersion force co-exists along with the main energy framework due to $\pi-\pi$ interactions which help to sustain the overall molecular packing of (I).

A structural analogue of (I) in the literature is the 2:1 co-crystal composed of two DTBA molecules and the isomeric 3-chlorobenzoic acid (3CBA) molecule, (II) (Tan & Tiekink, 2019b). Unlike (I), in which hydrogen bonds are formed

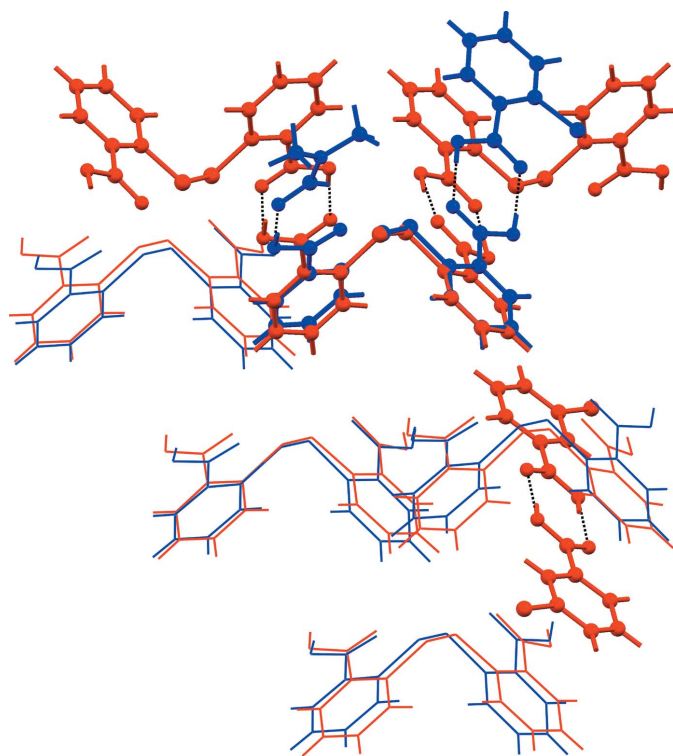


Figure 6
A comparison of the molecular packing between (I) (blue) and (II) (red), showing the similarity between five pairs of DTBA molecules with an overall r.m.s. deviation of 0.4 Å.

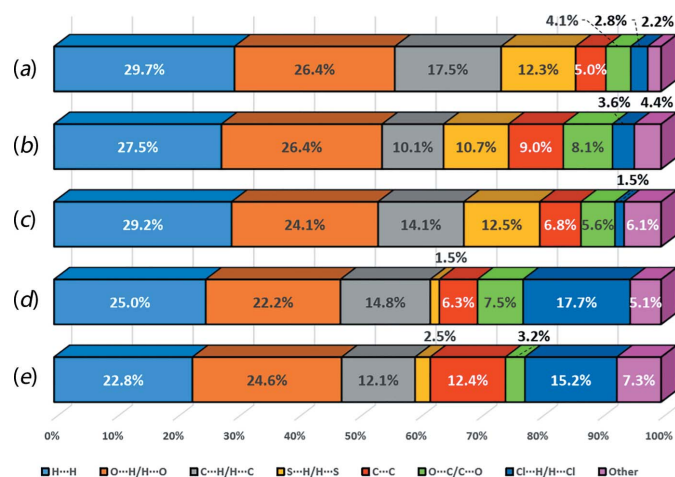


Figure 7
Percentage distribution of the corresponding close contacts to the Hirshfeld surfaces of (a) DTBA in (I), (b) first DTBA molecule in (II), (c) second DTBA molecule in (II), (d) 2CBA in (I) and (e) 3CBA in (II).

between DTBA, 2CBA and DMF to result in a three-molecule aggregate, Fig. 2(a), in (II) the two DTBA molecules (DTBA-IIa and DTBA-IIb) form hydrogen bonds with each other, to yield a non-symmetric homosynthon, and with the two remaining carboxylic acid groups being hydrogen bonded to two 3CBA molecules to give rise to a four-molecule aggregate.

A molecular cluster of (I) and (II) containing 20 molecules was subjected to molecular packing analysis using *Mercury* (Macrae *et al.*, 2006), with the geometric tolerances being set to the default values (20% for distance and 20° for angle tolerance); molecular inversions were allowed during the comparison. The study shows that there are five pairs of DTBA molecules from (I) and (II) which exhibit close similarity in the molecular packing with an r.m.s. deviation of 0.4 Å, Fig. 6.

Both (I) and (II) also exhibit similarity in terms of their close contacts as evidenced from the percentage contribution of the corresponding contacts obtained through Hirshfeld surface analysis for the DTBA molecules in (I) and (II), 2CBA in (I) or 3CBA in (II), Fig. 7. In general, the variations in contributions between those DTBA molecules as well as 2CBA and 3CBA are relatively small: these differences range from 0.2 to 2.9% and 1.0 to 2.7% respectively. Exceptions are noted in the $\text{C}\cdots\text{H}/\text{H}\cdots\text{C}$ contacts which contribute about 17.5% of the overall contacts in DTBA-I, that is about 7.4 and 3.4% higher than the contacts in DTBA-IIa and DTBA-IIb, respectively. On the other hand, a relatively higher contribution is observed for the $\text{C}\cdots\text{C}$ contacts in 3CBA (*ca* 12.4%) which is approximately 6% greater than 2CBA in (I) (*ca* 6.3%).

6. Database survey

There are over 200 structures included in the Cambridge Structural Database (version 5.40; Groom *et al.*, 2016) featuring hydrogen bonds between carboxylic acid residues and DMF. The most relevant structure is that of the 1:2

Table 3
Experimental details.

Crystal data	
Chemical formula	C ₁₄ H ₁₀ O ₄ S ₂ ·C ₇ H ₅ ClO ₂ ·C ₃ H ₇ NO
<i>M</i> _r	536.00
Crystal system, space group	Triclinic, <i>P</i> $\bar{1}$
Temperature (K)	100
<i>a</i> , <i>b</i> , <i>c</i> (Å)	7.7487 (3), 7.8575 (3), 21.4486 (6)
α , β , γ (°)	86.136 (3), 88.693 (2), 65.080 (4)
<i>V</i> (Å ³)	1181.61 (8)
<i>Z</i>	2
Radiation type	Cu <i>K</i> α
μ (mm ⁻¹)	3.50
Crystal size (mm)	0.19 × 0.12 × 0.03
Data collection	
Diffractometer	XtaLAB Synergy, Dualflex, AtlasS2
Absorption correction	Gaussian (<i>CrysAlis PRO</i> ; Rigaku OD, 2018)
<i>T</i> _{min} , <i>T</i> _{max}	0.413, 1.000
No. of measured, independent and observed [<i>I</i> > 2σ(<i>I</i>)] reflections	40239, 4915, 4507
<i>R</i> _{int}	0.057
(sin θ /λ) _{max} (Å ⁻¹)	0.630
Refinement	
<i>R</i> [<i>F</i> ² > 2σ(<i>F</i> ²)], <i>wR</i> (<i>F</i> ²), <i>S</i>	0.067, 0.203, 1.10
No. of reflections	4915
No. of parameters	330
H-atom treatment	H atoms treated by a mixture of independent and constrained refinement
$\Delta\rho_{\text{max}}$, $\Delta\rho_{\text{min}}$ (e Å ⁻³)	1.21, -0.83

Computer programs: *CrysAlis PRO* (Rigaku OD, 2018), *SHELXT* (Sheldrick, 2015b), *SHELXL* (Sheldrick, 2015a), *ORTEP-3 for Windows* (Farrugia, 2012), *OLEX2* (Dolomanov *et al.*, 2009) and *Mercury* (Macrae *et al.*, 2006) and *publCIF* (Westrip, 2010).

DTBA:DMF solvate (Cai *et al.*, 2006). Here, both carboxylic acid residues engage in hydrogen bonding interactions with DMF molecules akin to that seen in (I). There are approximately 250 structures where (non-coordinated) DMF and a carboxylic acid residue are present in the same crystal but no hydrogen bonding is evident between them. This suggests a 40% likelihood of hydrogen bonding between carboxylic acids and DMF, a percentage higher than for the formation of the eight-membered {···HOCO}₂ synthon in carboxylic acid structures, *i.e.* 33%, emphasizing that this particular synthon can be readily disrupted in the presence of competing synthons (Allen *et al.*, 1999).

7. Synthesis and crystallization

All chemical precursors were of reagent grade and used as received without further purification. 2-Mercaptobenzoic acid (Merck; 0.154 g, 0.001 mol) was mixed with 2-chlorobenzoic acid (Hopkin & Williams, 0.157 g, 0.001 mol) and ground for 15 mins in the presence of a few drops of methanol. The procedure was repeated three times. Colourless blocks were obtained through the careful layering of toluene (1 ml) on an *N,N*-dimethylformamide (1 ml) solution of the ground

mixture. M.p. 437.3–438.9 K. IR (cm⁻¹): 3076 ν(C–H), 1678 ν(C=O), 1473 ν(C=C), 1426 δ(C–H), 736 δ(C–Cl).

8. Refinement

Crystal data, data collection and structure refinement details are summarized in Table 3. The carbon-bound H atoms were placed in calculated positions (C–H = 0.93–0.96 Å) and were included in the refinement in the riding-model approximation, with *U*_{iso}(H) set to 1.2–1.5 *U*_{eq}(C). The oxygen-bound H atoms were located from difference Fourier maps and refined without constraint. Owing to poor agreement, one reflection, *i.e.* (4 2 2), was omitted from the final cycles of refinement.

Funding information

The support of Sunway University for studies in co-crystals, through Grant No. INT-FST-RCCM-2016-01, is gratefully acknowledged.

References

- Allen, F. H., Motherwell, W. D. S., Raithby, P. R., Shields, G. P. & Taylor, R. (1999). *New J. Chem.* **23**, 25–34.
- Broker, G. A. & Tiekink, E. R. T. (2007). *CrystEngComm*, **9**, 1096–1109.
- Cai, Y.-P., Sun, F., Zhu, L.-C., Yu, Q.-Y. & Liu, M.-S. (2006). *Acta Cryst. E* **62**, o841–o842.
- Dolomanov, O. V., Bourhis, L. J., Gildea, R. J., Howard, J. A. K. & Puschmann, H. (2009). *J. Appl. Cryst.* **42**, 339–341.
- Farrugia, L. J. (2012). *J. Appl. Cryst.* **45**, 849–854.
- Gorobet, A., Vitu, A., Petuhov, O. & Croitor, L. (2018). *Polyhedron*, **151**, 51–57.
- Grabowski, S. (2008). *J. Phys. Org. Chem.* **21**, 694–702.
- Groom, C. R., Bruno, I. J., Lightfoot, M. P. & Ward, S. C. (2016). *Acta Cryst. B* **72**, 171–179.
- Macrae, C. F., Edgington, P. R., McCabe, P., Pidcock, E., Shields, G. P., Taylor, R., Towler, M. & van de Streek, J. (2006). *J. Appl. Cryst.* **39**, 453–457.
- Nakanishi, W., Nakamoto, T., Hayashi, S., Sasamori, T. & Tokitoh, N. (2007). *Chem. Eur. J.* **13**, 255–268.
- Rigaku OD (2018). *CrysAlis PRO* Software system. Rigaku Oxford Diffraction, Oxford, UK.
- Rowland, C. E., Cantos, P. M., Toby, B. H., Frisch, M., Deschamps, J. R. & Cahill, C. L. (2011). *Cryst. Growth Des.* **11**, 1370–1374.
- Sheldrick, G. M. (2015a). *Acta Cryst. C* **71**, 3–8.
- Sheldrick, G. M. (2015b). *Acta Cryst. A* **71**, 3–8.
- Spartan'16 (2017). *Spartan'16*. Wavefunction, Inc. Irvine, CA.
- Spek, A. L. (2009). *Acta Cryst. D* **65**, 148–155.
- Tan, S. L., Jotani, M. M. & Tiekink, E. R. T. (2019). *Acta Cryst. E* **75**, 308–318.
- Tan, S. L. & Tiekink, E. R. T. (2018). *Acta Cryst. E* **74**, 1764–1771.
- Tan, S. L. & Tiekink, E. R. T. (2019a). *Acta Cryst. E* **75**, 1–7.
- Tan, S. L. & Tiekink, E. R. T. (2019b). *Z. Kristallogr. New Cryst. Struct.* **234** doi: 10.1515/ncrs-2018-0442.
- Tiekink, E. R. T. & Henderson, W. (2017). *Coord. Chem. Rev.* **341**, 19–52.
- Turner, M. J., Mckinnon, J. J., Wolff, S. K., Grimwood, D. J., Spackman, P. R., Jayatilaka, D. & Spackman, M. A. (2017). *Crystal Explorer 17*. The University of Western Australia.
- Wehr-Candler, T. & Henderson, W. (2016). *Coord. Chem. Rev.* **313**, 111–155.
- Westrip, S. P. (2010). *J. Appl. Cryst.* **43**, 920–925.

supporting information

Acta Cryst. (2019). E75, 475–481 [https://doi.org/10.1107/S205698901900375X]

A 1:1:1 co-crystal solvate comprising 2,2'-dithiodibenzoic acid, 2-chlorobenzoic acid and *N,N*-dimethylformamide: crystal structure, Hirshfeld surface analysis and computational study

Sang Loon Tan and Edward R. T. Tiekink

Computing details

Data collection: *CrysAlis PRO* (Rigaku OD, 2018); cell refinement: *CrysAlis PRO* (Rigaku OD, 2018); data reduction: *CrysAlis PRO* (Rigaku OD, 2018); program(s) used to solve structure: SHELXT (Sheldrick, 2015*b*); program(s) used to refine structure: SHELXL (Sheldrick, 2015*a*); molecular graphics: ORTEP-3 for Windows (Farrugia, 2012), OLEX2 (Dolomanov *et al.*, 2009) and Mercury (Macrae *et al.*, 2006); software used to prepare material for publication: publCIF (Westrip, 2010).

2,2'-Dithiodibenzoic acid–2-chlorobenzoic acid–*N,N*-dimethylformamide (1/1/1)

Crystal data

$C_{14}H_{10}O_4S_2 \cdot C_7H_5ClO_2 \cdot C_3H_7NO$

$M_r = 536.00$

Triclinic, $P\bar{1}$

$a = 7.7487$ (3) Å

$b = 7.8575$ (3) Å

$c = 21.4486$ (6) Å

$\alpha = 86.136$ (3)°

$\beta = 88.693$ (2)°

$\gamma = 65.080$ (4)°

$V = 1181.61$ (8) Å³

$Z = 2$

$F(000) = 556$

$D_x = 1.506$ Mg m⁻³

Cu $K\alpha$ radiation, $\lambda = 1.54184$ Å

Cell parameters from 21119 reflections

$\theta = 4.0$ – 76.1 °

$\mu = 3.50$ mm⁻¹

$T = 100$ K

Plate, colourless

$0.19 \times 0.12 \times 0.03$ mm

Data collection

XtaLAB Synergy, Dualflex, AtlasS2
diffractometer

Radiation source: micro-focus sealed X-ray
tube, PhotonJet (Cu) X-ray Source

Mirror monochromator

Detector resolution: 5.2558 pixels mm⁻¹

ω scans

Absorption correction: gaussian
(CrysAlisPro; Rigaku OD, 2018)

$T_{\min} = 0.413$, $T_{\max} = 1.000$

40239 measured reflections

4915 independent reflections

4507 reflections with $I > 2\sigma(I)$

$R_{\text{int}} = 0.057$

$\theta_{\max} = 76.1$ °, $\theta_{\min} = 4.1$ °

$h = -9 \rightarrow 9$

$k = -9 \rightarrow 9$

$l = -24 \rightarrow 26$

Refinement

Refinement on F^2

Least-squares matrix: full

$R[F^2 > 2\sigma(F^2)] = 0.067$

$wR(F^2) = 0.203$

$S = 1.10$

4915 reflections

330 parameters

0 restraints

Primary atom site location: dual

Hydrogen site location: mixed

H atoms treated by a mixture of independent
and constrained refinement
 $w = 1/[\sigma^2(F_o^2) + (0.1187P)^2 + 2.0348P]$
where $P = (F_o^2 + 2F_c^2)/3$

$$(\Delta/\sigma)_{\max} = 0.001$$

$$\Delta\rho_{\max} = 1.21 \text{ e } \text{\AA}^{-3}$$

$$\Delta\rho_{\min} = -0.83 \text{ e } \text{\AA}^{-3}$$

Special details

Geometry. All esds (except the esd in the dihedral angle between two l.s. planes) are estimated using the full covariance matrix. The cell esds are taken into account individually in the estimation of esds in distances, angles and torsion angles; correlations between esds in cell parameters are only used when they are defined by crystal symmetry. An approximate (isotropic) treatment of cell esds is used for estimating esds involving l.s. planes.

Fractional atomic coordinates and isotropic or equivalent isotropic displacement parameters (\AA^2)

	<i>x</i>	<i>y</i>	<i>z</i>	$U_{\text{iso}}^*/U_{\text{eq}}$
S1	0.59149 (11)	0.53119 (12)	0.76852 (4)	0.0306 (2)
Cl1	0.45069 (12)	0.95992 (13)	1.14356 (4)	0.0349 (2)
S2	0.59937 (12)	0.53437 (12)	0.67272 (4)	0.0308 (2)
O4	0.3171 (4)	0.6699 (4)	0.95268 (11)	0.0326 (5)
H4O	0.364 (8)	0.709 (7)	0.973 (3)	0.052 (15)*
O3	0.5740 (3)	0.5927 (3)	0.89192 (10)	0.0296 (5)
O2	0.7735 (4)	0.6833 (4)	0.97404 (12)	0.0354 (6)
H2O	0.712 (8)	0.652 (8)	0.950 (3)	0.060 (16)*
O1	0.5007 (3)	0.7890 (4)	1.02638 (11)	0.0344 (6)
O5	0.6630 (4)	0.5440 (4)	0.55037 (12)	0.0418 (6)
O6	0.8588 (4)	0.3049 (4)	0.49649 (12)	0.0410 (6)
H6O	0.841 (7)	0.395 (7)	0.468 (2)	0.045 (13)*
O7	0.8389 (4)	0.5600 (4)	0.41008 (12)	0.0434 (6)
N1	0.7396 (5)	0.8751 (5)	0.39798 (14)	0.0400 (7)
C9	0.2951 (5)	0.5828 (4)	0.85135 (15)	0.0267 (6)
C1	0.6657 (5)	0.7680 (5)	1.02109 (15)	0.0275 (6)
C14	0.3607 (5)	0.5473 (5)	0.78952 (15)	0.0270 (6)
C8	0.4089 (4)	0.6141 (5)	0.90013 (15)	0.0267 (6)
C2	0.7656 (5)	0.8312 (5)	1.06648 (15)	0.0280 (6)
C12	0.0633 (5)	0.5400 (5)	0.76228 (16)	0.0306 (7)
H12	−0.016266	0.526211	0.731834	0.037*
C10	0.1132 (5)	0.5965 (5)	0.86691 (15)	0.0291 (7)
H10	0.068160	0.622104	0.908335	0.035*
C13	0.2422 (5)	0.5262 (5)	0.74536 (15)	0.0295 (7)
H13	0.284561	0.502362	0.703600	0.035*
C6	0.7871 (5)	0.9609 (5)	1.16394 (16)	0.0323 (7)
H6A	0.730171	1.015228	1.201643	0.039*
C11	−0.0011 (5)	0.5736 (5)	0.82314 (16)	0.0318 (7)
H11	−0.123116	0.580647	0.834470	0.038*
C5	0.9736 (5)	0.9304 (5)	1.15083 (17)	0.0345 (7)
H5	1.044152	0.963015	1.179689	0.041*
C7	0.6831 (5)	0.9126 (5)	1.12226 (15)	0.0274 (6)
C16	0.6785 (5)	0.1584 (5)	0.70069 (16)	0.0338 (7)
H16	0.626413	0.196047	0.740635	0.041*
C15	0.6826 (5)	0.2925 (5)	0.65578 (16)	0.0312 (7)

C21	0.7543 (5)	0.3771 (5)	0.54597 (16)	0.0336 (7)
C20	0.7578 (5)	0.2356 (5)	0.59629 (16)	0.0330 (7)
C3	0.9540 (5)	0.8034 (5)	1.05434 (17)	0.0319 (7)
H3	1.012239	0.749575	1.016708	0.038*
C22	0.7667 (6)	0.7194 (5)	0.42990 (18)	0.0413 (9)
H22	0.727643	0.728713	0.472319	0.050*
C17	0.7494 (6)	−0.0294 (5)	0.68806 (18)	0.0402 (8)
H17	0.743500	−0.119055	0.719045	0.048*
C19	0.8321 (6)	0.0448 (5)	0.58490 (18)	0.0398 (8)
H19	0.885722	0.005247	0.545262	0.048*
C4	1.0573 (5)	0.8524 (5)	1.09581 (18)	0.0368 (8)
H4A	1.184608	0.832653	1.086567	0.044*
C18	0.8290 (6)	−0.0872 (5)	0.63029 (19)	0.0432 (9)
H18	0.880856	−0.216500	0.622025	0.052*
C23	0.7881 (7)	0.8803 (6)	0.33196 (18)	0.0441 (9)
H23A	0.854211	0.962019	0.324500	0.066*
H23B	0.671435	0.929459	0.306655	0.066*
H23C	0.871087	0.752967	0.320389	0.066*
C24	0.6454 (7)	1.0572 (6)	0.4254 (2)	0.0487 (10)
H24A	0.626207	1.037588	0.470118	0.073*
H24B	0.521838	1.129721	0.404825	0.073*
H24C	0.724883	1.126361	0.419463	0.073*

Atomic displacement parameters (Å²)

	U^{11}	U^{22}	U^{33}	U^{12}	U^{13}	U^{23}
S1	0.0263 (4)	0.0454 (5)	0.0243 (4)	−0.0182 (3)	0.0065 (3)	−0.0111 (3)
Cl1	0.0324 (4)	0.0482 (5)	0.0290 (4)	−0.0208 (4)	0.0096 (3)	−0.0119 (3)
S2	0.0342 (4)	0.0354 (4)	0.0240 (4)	−0.0152 (3)	0.0080 (3)	−0.0083 (3)
O4	0.0306 (12)	0.0483 (14)	0.0260 (12)	−0.0220 (11)	0.0055 (9)	−0.0132 (10)
O3	0.0229 (11)	0.0420 (13)	0.0266 (11)	−0.0153 (10)	0.0053 (8)	−0.0106 (9)
O2	0.0300 (12)	0.0515 (15)	0.0287 (12)	−0.0195 (11)	0.0069 (10)	−0.0152 (11)
O1	0.0266 (12)	0.0495 (15)	0.0309 (12)	−0.0180 (11)	0.0065 (9)	−0.0158 (10)
O5	0.0530 (16)	0.0358 (14)	0.0291 (13)	−0.0115 (12)	0.0136 (11)	−0.0056 (10)
O6	0.0519 (16)	0.0363 (13)	0.0284 (13)	−0.0123 (12)	0.0155 (11)	−0.0069 (11)
O7	0.0574 (17)	0.0385 (14)	0.0313 (13)	−0.0169 (12)	0.0120 (12)	−0.0081 (11)
N1	0.0502 (19)	0.0412 (17)	0.0297 (15)	−0.0200 (15)	0.0053 (13)	−0.0058 (13)
C9	0.0266 (15)	0.0296 (15)	0.0242 (15)	−0.0117 (12)	0.0016 (12)	−0.0056 (12)
C1	0.0259 (15)	0.0313 (16)	0.0251 (15)	−0.0113 (12)	0.0035 (12)	−0.0059 (12)
C14	0.0255 (15)	0.0305 (15)	0.0267 (15)	−0.0127 (12)	0.0046 (12)	−0.0077 (12)
C8	0.0252 (15)	0.0316 (16)	0.0250 (15)	−0.0131 (12)	0.0034 (12)	−0.0067 (12)
C2	0.0254 (15)	0.0316 (16)	0.0257 (15)	−0.0105 (12)	0.0019 (12)	−0.0040 (12)
C12	0.0279 (16)	0.0355 (17)	0.0302 (16)	−0.0141 (13)	−0.0001 (13)	−0.0082 (13)
C10	0.0280 (16)	0.0349 (17)	0.0262 (16)	−0.0143 (13)	0.0054 (12)	−0.0082 (13)
C13	0.0278 (16)	0.0372 (17)	0.0242 (15)	−0.0136 (13)	0.0031 (12)	−0.0080 (13)
C6	0.0353 (18)	0.0357 (17)	0.0248 (16)	−0.0134 (14)	−0.0001 (13)	−0.0042 (13)
C11	0.0255 (16)	0.0386 (18)	0.0332 (17)	−0.0145 (14)	0.0034 (13)	−0.0097 (14)
C5	0.0334 (18)	0.0379 (18)	0.0333 (18)	−0.0152 (14)	−0.0034 (14)	−0.0062 (14)

C7	0.0269 (15)	0.0302 (15)	0.0250 (15)	−0.0118 (12)	0.0033 (12)	−0.0042 (12)
C16	0.0318 (17)	0.0385 (18)	0.0274 (16)	−0.0109 (14)	0.0060 (13)	−0.0057 (13)
C15	0.0268 (16)	0.0368 (17)	0.0273 (16)	−0.0102 (13)	0.0042 (12)	−0.0076 (13)
C21	0.0359 (18)	0.0390 (18)	0.0255 (16)	−0.0146 (15)	0.0080 (13)	−0.0095 (13)
C20	0.0335 (17)	0.0372 (18)	0.0264 (16)	−0.0125 (14)	0.0052 (13)	−0.0062 (13)
C3	0.0259 (16)	0.0387 (18)	0.0331 (17)	−0.0142 (14)	0.0042 (13)	−0.0125 (14)
C22	0.046 (2)	0.040 (2)	0.0353 (19)	−0.0148 (17)	0.0088 (16)	−0.0088 (15)
C17	0.043 (2)	0.0355 (18)	0.0367 (19)	−0.0116 (16)	0.0097 (15)	−0.0009 (15)
C19	0.044 (2)	0.0384 (19)	0.0321 (18)	−0.0115 (16)	0.0110 (15)	−0.0099 (15)
C4	0.0259 (16)	0.046 (2)	0.0392 (19)	−0.0151 (15)	0.0014 (14)	−0.0108 (16)
C18	0.052 (2)	0.0323 (18)	0.040 (2)	−0.0119 (16)	0.0109 (17)	−0.0082 (15)
C23	0.060 (3)	0.048 (2)	0.0304 (18)	−0.028 (2)	0.0074 (17)	−0.0047 (16)
C24	0.061 (3)	0.038 (2)	0.041 (2)	−0.0153 (19)	0.0057 (19)	−0.0063 (17)

Geometric parameters (Å, °)

S1—S2	2.0531 (11)	C13—H13	0.9500
S1—C14	1.788 (3)	C6—H6A	0.9500
Cl1—C7	1.736 (3)	C6—C5	1.387 (5)
S2—C15	1.791 (4)	C6—C7	1.389 (5)
O4—H4O	0.74 (6)	C11—H11	0.9500
O4—C8	1.317 (4)	C5—H5	0.9500
O3—C8	1.229 (4)	C5—C4	1.384 (5)
O2—H2O	0.82 (6)	C16—H16	0.9500
O2—C1	1.320 (4)	C16—C15	1.389 (5)
O1—C1	1.222 (4)	C16—C17	1.384 (5)
O5—C21	1.209 (4)	C15—C20	1.411 (5)
O6—H6O	0.87 (5)	C21—C20	1.488 (5)
O6—C21	1.326 (4)	C20—C19	1.398 (5)
O7—C22	1.238 (5)	C3—H3	0.9500
N1—C22	1.298 (5)	C3—C4	1.385 (5)
N1—C23	1.459 (5)	C22—H22	0.9500
N1—C24	1.463 (5)	C17—H17	0.9500
C9—C14	1.412 (4)	C17—C18	1.388 (5)
C9—C8	1.480 (4)	C19—H19	0.9500
C9—C10	1.402 (5)	C19—C18	1.381 (6)
C1—C2	1.489 (5)	C4—H4A	0.9500
C14—C13	1.398 (5)	C18—H18	0.9500
C2—C7	1.404 (4)	C23—H23A	0.9800
C2—C3	1.403 (5)	C23—H23B	0.9800
C12—H12	0.9500	C23—H23C	0.9800
C12—C13	1.386 (5)	C24—H24A	0.9800
C12—C11	1.389 (5)	C24—H24B	0.9800
C10—H10	0.9500	C24—H24C	0.9800
C10—C11	1.376 (5)		
C14—S1—S2	105.47 (11)	C6—C7—C2	120.5 (3)
C15—S2—S1	104.62 (12)	C15—C16—H16	119.5

C8—O4—H4O	113 (4)	C17—C16—H16	119.5
C1—O2—H2O	110 (4)	C17—C16—C15	120.9 (3)
C21—O6—H6O	109 (3)	C16—C15—S2	121.2 (3)
C22—N1—C23	122.3 (3)	C16—C15—C20	119.1 (3)
C22—N1—C24	121.4 (3)	C20—C15—S2	119.7 (3)
C23—N1—C24	116.1 (3)	O5—C21—O6	123.2 (3)
C14—C9—C8	122.3 (3)	O5—C21—C20	122.2 (3)
C10—C9—C14	119.3 (3)	O6—C21—C20	114.6 (3)
C10—C9—C8	118.4 (3)	C15—C20—C21	120.5 (3)
O2—C1—C2	113.6 (3)	C19—C20—C15	119.0 (3)
O1—C1—O2	122.2 (3)	C19—C20—C21	120.5 (3)
O1—C1—C2	124.2 (3)	C2—C3—H3	119.2
C9—C14—S1	120.0 (2)	C4—C3—C2	121.7 (3)
C13—C14—S1	120.9 (2)	C4—C3—H3	119.2
C13—C14—C9	119.0 (3)	O7—C22—N1	125.9 (4)
O4—C8—C9	114.4 (3)	O7—C22—H22	117.0
O3—C8—O4	122.8 (3)	N1—C22—H22	117.0
O3—C8—C9	122.8 (3)	C16—C17—H17	119.9
C7—C2—C1	123.4 (3)	C16—C17—C18	120.2 (3)
C3—C2—C1	118.8 (3)	C18—C17—H17	119.9
C3—C2—C7	117.8 (3)	C20—C19—H19	119.4
C13—C12—H12	119.6	C18—C19—C20	121.1 (3)
C13—C12—C11	120.9 (3)	C18—C19—H19	119.4
C11—C12—H12	119.6	C5—C4—C3	119.5 (3)
C9—C10—H10	119.5	C5—C4—H4A	120.3
C11—C10—C9	121.1 (3)	C3—C4—H4A	120.3
C11—C10—H10	119.5	C17—C18—H18	120.2
C14—C13—H13	119.9	C19—C18—C17	119.5 (4)
C12—C13—C14	120.3 (3)	C19—C18—H18	120.2
C12—C13—H13	119.9	N1—C23—H23A	109.5
C5—C6—H6A	119.8	N1—C23—H23B	109.5
C5—C6—C7	120.4 (3)	N1—C23—H23C	109.5
C7—C6—H6A	119.8	H23A—C23—H23B	109.5
C12—C11—H11	120.3	H23A—C23—H23C	109.5
C10—C11—C12	119.4 (3)	H23B—C23—H23C	109.5
C10—C11—H11	120.3	N1—C24—H24A	109.5
C6—C5—H5	119.9	N1—C24—H24B	109.5
C4—C5—C6	120.2 (3)	N1—C24—H24C	109.5
C4—C5—H5	119.9	H24A—C24—H24B	109.5
C2—C7—C11	123.5 (3)	H24A—C24—H24C	109.5
C6—C7—C11	116.0 (3)	H24B—C24—H24C	109.5
S1—S2—C15—C16	17.0 (3)	C2—C3—C4—C5	0.2 (6)
S1—S2—C15—C20	−161.5 (3)	C10—C9—C14—S1	179.5 (3)
S1—C14—C13—C12	−179.7 (3)	C10—C9—C14—C13	−0.2 (5)
S2—S1—C14—C9	−168.5 (2)	C10—C9—C8—O4	−6.1 (4)
S2—S1—C14—C13	11.1 (3)	C10—C9—C8—O3	175.0 (3)
S2—C15—C20—C21	−4.9 (5)	C13—C12—C11—C10	1.1 (5)

S2—C15—C20—C19	176.4 (3)	C6—C5—C4—C3	−0.7 (6)
O2—C1—C2—C7	−175.4 (3)	C11—C12—C13—C14	−0.4 (5)
O2—C1—C2—C3	2.5 (5)	C5—C6—C7—C11	−179.4 (3)
O1—C1—C2—C7	3.7 (5)	C5—C6—C7—C2	0.3 (5)
O1—C1—C2—C3	−178.3 (3)	C7—C2—C3—C4	0.5 (5)
O5—C21—C20—C15	−11.7 (6)	C7—C6—C5—C4	0.4 (6)
O5—C21—C20—C19	167.0 (4)	C16—C15—C20—C21	176.5 (3)
O6—C21—C20—C15	168.3 (3)	C16—C15—C20—C19	−2.1 (5)
O6—C21—C20—C19	−13.0 (5)	C16—C17—C18—C19	−1.8 (7)
C9—C14—C13—C12	0.0 (5)	C15—C16—C17—C18	1.1 (6)
C9—C10—C11—C12	−1.3 (5)	C15—C20—C19—C18	1.5 (6)
C1—C2—C7—C11	−3.2 (5)	C21—C20—C19—C18	−177.2 (4)
C1—C2—C7—C6	177.1 (3)	C20—C19—C18—C17	0.5 (7)
C1—C2—C3—C4	−177.5 (3)	C3—C2—C7—C11	178.9 (3)
C14—C9—C8—O4	171.4 (3)	C3—C2—C7—C6	−0.8 (5)
C14—C9—C8—O3	−7.5 (5)	C17—C16—C15—S2	−177.6 (3)
C14—C9—C10—C11	0.8 (5)	C17—C16—C15—C20	0.9 (5)
C8—C9—C14—S1	2.1 (4)	C23—N1—C22—O7	1.9 (7)
C8—C9—C14—C13	−177.6 (3)	C24—N1—C22—O7	177.4 (4)
C8—C9—C10—C11	178.4 (3)		

Hydrogen-bond geometry (Å, °)

<i>D</i> —H \cdots <i>A</i>	<i>D</i> —H	H \cdots <i>A</i>	<i>D</i> \cdots <i>A</i>	<i>D</i> —H \cdots <i>A</i>
O2—H2O \cdots O3	0.83 (6)	1.86 (7)	2.687 (4)	176 (9)
O4—H4O \cdots O1	0.73 (7)	1.88 (6)	2.612 (4)	175 (5)
O6—H6O \cdots O7	0.87 (5)	1.73 (5)	2.594 (4)	172 (5)
C3—H3 \cdots O4 ⁱ	0.95	2.57	3.363 (5)	142
C10—H10 \cdots O2 ⁱⁱ	0.95	2.54	3.331 (5)	141
C11—H11 \cdots S1 ⁱⁱ	0.95	2.83	3.544 (4)	133
C22—H22 \cdots O5	0.95	2.33	3.095 (5)	138
C24—H24B \cdots S2 ⁱⁱⁱ	0.98	2.83	3.531 (4)	129

Symmetry codes: (i) $x-1, y, z$; (ii) $x+1, y, z$; (iii) $-x+1, -y, -z+1$.